Mechanical Systems and Signal Processing 204 (2023) 110773

Contents lists available at ScienceDirect

Mechanical Systems and Signal Processing

journal homepage: www.elsevier.com/locate/ymssp

Early detection of tool wear in electromechanical broaching machines by monitoring main stroke servomotors

Iñigo Aldekoa [a,*], Ander del Olmo [a], Leonardo Sastoque-Pinilla [a,b], Sara Sendino-Mouliet [a,b], Unai Lopez-Novoa [c], Luis Norberto López de Lacalle [a,b]

[a] Advanced Manufacturing Centre for Aeronautics (CFAA), University of the Basque Country (UPV/EHU), Biscay Science and Technology Park, Ed.202, Zamudio, 48017, Biscay, Spain

[b] Department of Mechanical Engineering, University of the Basque Country (UPV/EHU), Torres Quevedo Sq, Bilbao, 48013, Biscay, Spain

[c] Department of Computer Languages and Systems, University of the Basque Country (UPV/EHU), Rafael Moreno St, 2-3, Bilbao, 48013, Biscay, Spain

ARTICLE INFO

Communicated by Y. Lei

Keywords:
Broaching process
Process monitoring
Tool wear estimation
Sensorless approach

ABSTRACT

This paper aims to provide researchers and engineers with evidence that sensorless machine variable monitoring can achieve tool wear monitoring in broaching in real production environments, reducing production errors, enhancing product quality, and facilitating zero-defect manufacturing. Additionally, broaching plays a crucial role in improving the quality of manufacturing products and processes. These aspects are especially pertinent in aeronautical manufacturing, which serves as the experimental case in this study.

The research presents findings that establish a correlation between the variables of a broaching machine's servomotors and the condition of the broaching tools. The authors propose an effective method for measuring broaching tool wear without external sensors and provide a detailed explanation of the methodology, enabling reproducibility of similar results. The results stem from three trials conducted on an electromechanical vertical broaching machine, utilizing cemented carbide grade broaching tools to broach a superalloy Inconel 718 test piece. The machine data collected facilitated the training of a set of machine learning models, accurately estimating tool wear on the broaches. Each model demonstrates high predictive accuracy, with a coefficient of determination surpassing 0.9.

1. Introduction

The substantial increase in worldwide mobility, especially in the aeronautical sector, has significantly impacted many fields of industry and the production of aircraft engines counts among the sectors affected most by this trend [1]. This includes the broaching of turbine disks, considered one of the most challenging aspects of turbomachinery production due to its complexity. As a result, the highest quality standards are implemented to ensure safety-critical reliability [1,2].

Broaching is a cutting process widely used in the manufacturing of numerous parts with complex internal and external profiles, high surface integrity, and accuracy requirements, such as turbine disks, that cannot be achieved using flexible metal cutting techniques [2,3]. As Axinte and Gindy [3] mentioned, broaching is typically the last machining step in the manufacturing process of components, so, the process output is crucial in terms of surface quality and integrity.

* Corresponding author.
E-mail address: inigo.aldekoa@ehu.eus (I. Aldekoa).

https://doi.org/10.1016/j.ymssp.2023.110773
Received 20 March 2023; Received in revised form 27 July 2023; Accepted 9 September 2023
Available online 28 September 2023

Nomenclature

CNC	Computer numerical control
CSV	Comma-separated values
$KNNR$	K-nearest neighbors regressor
MAE	Mean absolute error
MSE	Mean squared error
PLC	Programmable logic computer
RBF	Radial basis function
RFR	Random forest regressor
$RMSE$	Root mean squared error
$SVMR$	Support vector machine regressor
Vc	Cutting speed [m/min]

Actual manufacturing demands a well-supervised operation with a focus on the broaching tool condition in order to achieve excellent quality and productivity [4,5]. To reach the level of surface integrity required for aircraft engine components, the condition of the broaching tool is a major factor, especially in the aero-engines' moving components [3,6]. The exceptional strength and corrosion resistance of super-alloys such as Inconel 718, Waspaloy, Rene 104, and IN100 PM causes rapid wear on cutting tools [7–9], requiring frequent replacement or resharpening. Thermal fracturing, attrition, abrasion, plastic deformation, diffusion, and substrate grain pull-out are some of the main causes of tool wear [10,11]. Therefore, using worn tools can lead to decreased dimensional accuracy, surface quality of produced components, and process stability due to vibrations [4]. Consequently, the integration of a tool wear monitoring system in the machining of super-alloys is strongly recommended to improve quality and productivity, and the automation of tool condition detection and categorization is of great importance in the practical industrial environment [12]. However, despite the significant investment in tools and the high value of machined parts, limited research has been conducted on monitoring the broaching process.

As one of the pioneers investigating this issue in broaching, Budak [13] proposed a monitoring system to assess broaching process performance by monitoring forces and power signals. His study revealed that internal broaching exhibited non-uniform load distribution across the tool section, leading to uneven wear. Additionally, Budak demonstrated that force sensor outputs in broaching heavily depend on the part, tool, and fixture geometry, making them impractical to calibrate for various conditions. Consequently, further development is required before they can be implemented in production. Nevertheless, these sensors are still valuable for obtaining a reference force value when the broaching tools are sharp and detecting any non-monotonic increase indicative of wear.

Similarly, Axinte and Gindy [3] conducted research to monitor the progression of broaching tool wear evaluating different sensor types to identify a suitable monitoring technique. Cutting force signals have exhibited excellent sensitivity to changes in tool condition; however, their drawback lies in the need to install a force measuring device on existing broaching machines. Vibrations and acoustic emission (AE) sensors, on the other hand, can be easily positioned and their signals can be correlated with tool condition. However, due to susceptibility to noise generated by mechanical and hydraulic components, these signals require meticulous processing to filter out unwanted interference. Ultimately, the authors concluded that power monitoring may be a viable option for mechanically powered broaching machines, whereas pressure monitoring is not suitable for hydraulically powered broaching.

In more recent research, Bediaga et al. [14] proposed a comprehensive approach to broaching tool monitoring, focusing on advanced signal treatment. They emphasize the importance of removing all harmonics unrelated to the tooth passing frequency to ensure accurate force measurements. Their findings highlighted an increase in axial force peaks and the corresponding increase in machine energy consumption with tool wear.

The most recent systematic review of tool condition monitoring (TCM) methods [15] confirms that the most common approach for tool wear monitoring is to analyze multiple process signals. Sensorless monitoring techniques that use internal machine data have become popular due to the cost and potential impact on the machining process of installing external sensors. These methods eliminate the need for sensor calibration and external sensor investments.

Implementing an appropriate tool wear monitoring system can accurately evaluate the rate of tool wear and prompt tool replacement to avoid the rejection of critical components. Additionally, accurate tool wear estimation can significantly increase tool life and cost-effectiveness through broaching tool regrinding.

One of the top research priorities in the academic community and the aero-engine industry is the development of broadly applicable machining process monitoring systems. Shi et al. [16] stated that process monitoring systems are expected to provide a number of major benefits, such as preserving machine tool reliability and in-process sensing of product quality. The time- and frequency-domain analysis of output signals demonstrates the variety of sensors and signal processing methods that can be used for broaching TCM [3]. However, as mentioned before, the proposed approach presented in this paper uses only the signals provided by the machine, which limits the scope of the variables that can be analyzed but provides ground for making a TCM system more accesible.

The merging of different datasets from various sources in the manufacturing process presents a significant challenge due to the abundance of information collected. Artificial intelligence (AI) methods have been increasingly used in machining processes in recent years to improve monitoring. Ongoing research aims to incorporate data-driven models into the cutting process to improve the prediction of crucial nonlinear issues, such as condition monitoring (CM), chatter, quality, modeling, and energy consumption [17]. In this context, process parameters such as temperature, vibrations, acceleration, and tool wear are monitored either through sensors or machine control data, which are then fed to machine learning (ML) or deep learning (DL) algorithms for prediction purposes. This approach allows for the accurate determination of the optimal time for tool replacement and minimizes downtime caused by critical failures. Additionally, other techniques such as TCM and CM, which are related to the current machining structure, can also be employed in this context.

Numerous studies have extensively analysed various ML algorithms to understand their strengths and weaknesses in adressing different machining problems. Existing tool condition recognition models are often based on general or specific machining processes, which limits their practical applicability to real-world scenarios. Additionally, the learning algorithms used in these models typically require a large amount of carefully selected training data to achieve high accuracy [18].

Lee et al. [19] used AI technology and DL techniques to accurately identify the condition of grinding wheels using machining sound. They successfully developed a convolutional neural network (CNN) architecture that achieved an impressive model performance with 97.44% accuracy and 98.26% precision.

Similar studies have been conducted to estimate tool wear conditions using various methods. Wu et al. [20] specifically investigated different ML algorithms, including random forest (RF), artificial neural network (ANN), and support vector regression (SVR), for tool wear monitoring. Their evaluation of benchmark data revealed that the RF-based prognostic method outperformed the ANN and SVR approaches in terms of generating more accurate predictions.

Cho et al. [21] developed an intelligent tool breakage detection system using the support vector machines (SVMs) to monitor cutting forces and power consumption in end milling processes. They successfully applied SVMs to predict wear progression and estimate the remaining useful life (RUL) of cutting tools. In another study, Benkedjouh et al. [22] presented a method for tool wear assessment and RUL prediction using SVMs. Experimental results demonstrated that SVMs effectively estimated wear progression and predicted the RUL of cutting tools.

Kilundu et al. [23] conducted a thorough examination, comparing different sources of process signals to identify tool wear conditions using various ML techniques, including bayesian networks, K-nearest neighbor (KNN), decision trees, and neural networks. The results revealed excellent tool wear classification performance for all methods, except for Bayesian networks, which exhibited poor classification for several instances.

In this work, two trials, with approximately 500 broaching strokes each, were conducted in a near-real production environment for tool wear monitoring, finding correlations and creating models. These trials have very similar characteristics and were conducted with the same set-up, so both of the trials' data can be used for the same analysis.

Considering all the reasons mentioned above, this study is centered on the identification of variables that facilitate the early detection of wear in broaching through indirect monitoring [24]. This article completes the description of Del Olmo et al. [25] with ML analysis and the effect of broaching tool rounding edge approach in Pérez-Salinas et al. [26].

The remainder of this paper is structured as follows: Section 2 provides the details about the machine configuration, workpiece and tools used in the trials. Following this, Section 3 presents the method for tool wear monitoring, detailing the procedure followed step by step. Then, Section 4 displays and reviews the outcome of the trials applying the method presented before. Finally, the conclusions are presented in Section 5.

2. Experimental framework

This section provides a detailed explanation of the machine configuration, data acquisition architecture, workpiece, and tools used in the experiments. The purpose of this setup was to conduct broaching tests, collect process data, and apply ML techniques to estimate the tool wear of each cutting edge.

2.1. Machine configuration

The broaching tests are carried out on an electromechanical broaching machine for external surfaces of the company EKIN®, model A218/RASHEM, shown in Fig. 1. Unlike other broaching machines, the cutting tool remains static on this machine. At the same time, the rotary indexing table, along with the workpiece, moves along the entire machine's Z-axis, allowing a higher cutting speed (Vc). Additionally, electromechanical broaching machines have excellent process capability and accuracy compared to other machines [27]. Notably, this machine's best feature is the possibility of extracting motor information and monitoring the cutting process.

The primary motion of the broaching machine is facilitated by two FKM85 AC brushless servomotors, which are three-phase servomotors connected in a star configuration (400 V). These servomotors are ideal for broaching processes due to their high efficiency, low starting current, and ability to maintain a consistent speed, ensuring high reliability and efficiency. To elevate the working table, the servomotors work in conjunction with a rack and pinion mechanism that transforms the rotatory motion into linear motion. Additionally, a reduction gearbox is incorporated to reduce the rotation speed of the pinion and increase the available torque, ensuring smooth operation of the device. Each AC servomotor has an incremental rotary encoder that measures its rotation and angular position, converting the rotatory motion into digital signals (see Fig. 2).

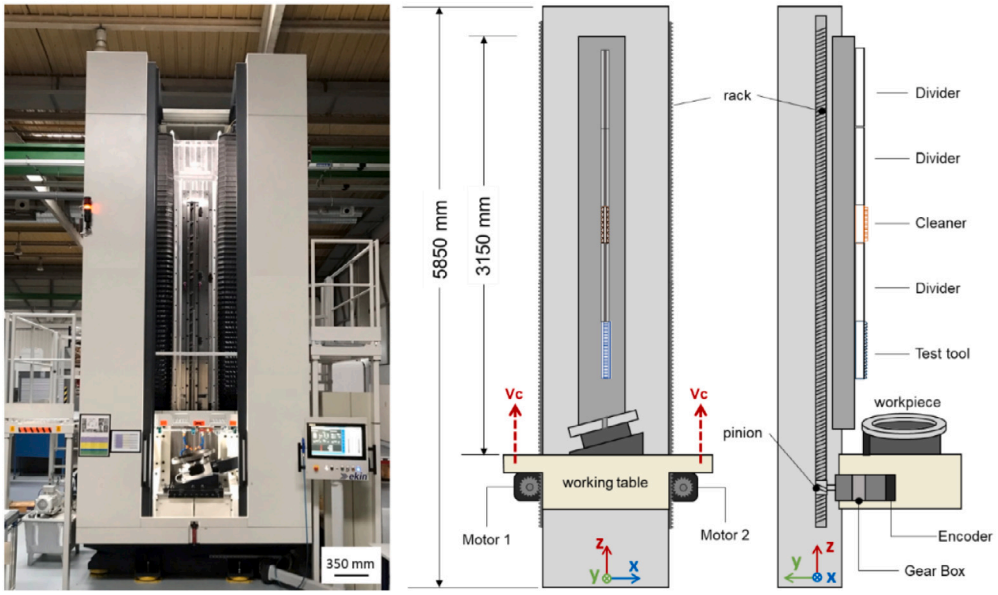

Fig. 1. Configuration and characteristics of the A218/RASHEM Electromechanical broaching machine used.

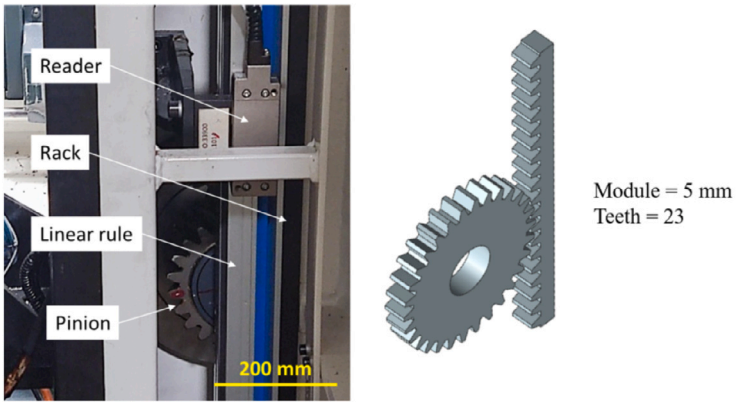

Fig. 2. Rack-pinion mechanism, linear rule and reader.

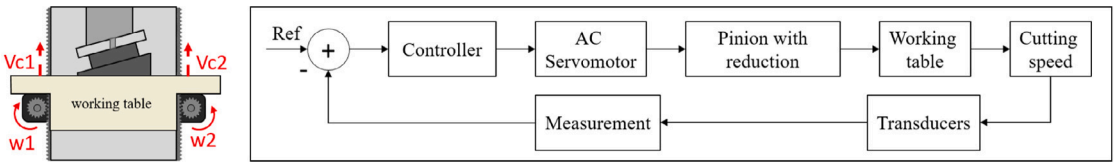

Fig. 3. Diagram of the working table and the control loop of Vc.

The entire system is controlled by computer numerical control (CNC) software, FAGOR® 8070, which controls the cutting process. In this case, the CNC is programmed to maintain a constant Vc throughout the cutting process. To achieve this, the system's control loop is closed every 4 ms (250 Hz), which allows the system to overcome the resistance of the material being machined, which could reduce the Vc. Adittionally, this allows for the collection of data about the engine condition at a lower or at least the same frequency as the control loop is closed (see Fig. 3).

During the tests, a program reads the CNC variables and values defined within the programmable logic controller (PLC), such as the servomotors' power, torque, temperature, and current, and extracts the data. The data is then collected in a data lake (a centralized repository in a private cloud where both structured and unstructured data are stored) [28,29]. This process is achieved using an edge device which collects data from the CNC, formats it as comma-separated values (CSV) files, and pushes them to the

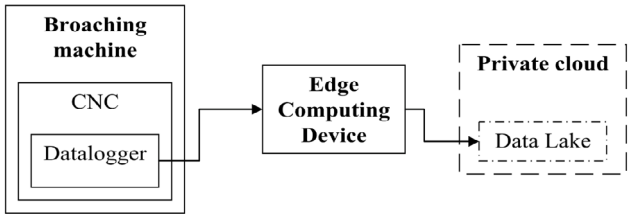

Fig. 4. Flowchart of the data architecture used in the broaching machine.

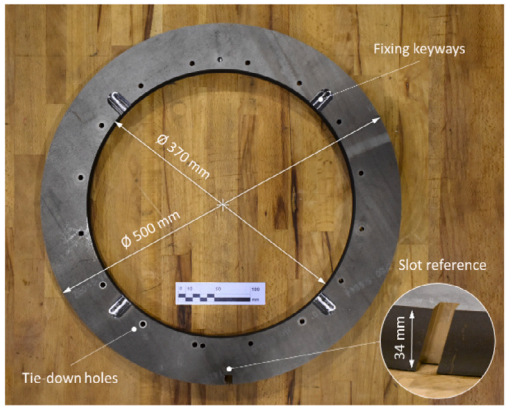

Fig. 5. Inconel 718 workpiece disk.

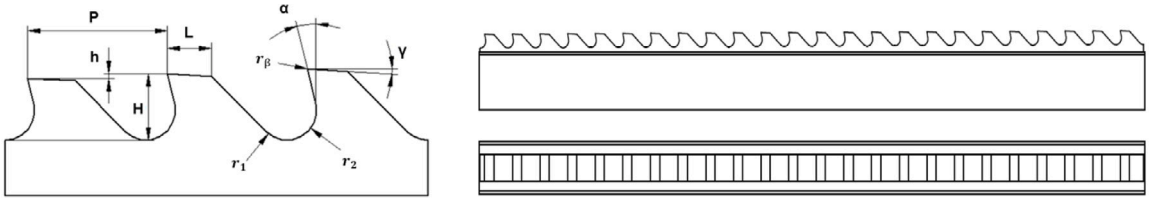

Fig. 6. Broaching tool diagram.

data lake. The edge device used in this work is a Savvy Smart Box developed by Savvy Data Systems [30]. A schema of the data collection process is depicted in Fig. 4.

2.2. Workpiece

The test piece shown in Fig. 5 comprises nickel-based superalloy Inconel 718, a material commonly used in the aerospace industry to manufacture aeroplane engine turbine disks [9,31]. Its dimensions can be seen in Fig. 5. This material was choosen for its excellent mechanical properties at high temperatures (around 850 K), as well as fatigue, creep and corrosion resistance [9,32]. However, its high strength and hardness also make it a challenging material to machine, resulting in high cutting forces and rapid tool wear.

2.3. Tools

Two roughing broaching tools of similar quality and identical geometry were selected for the high-performance machining of titanium and nickel base superalloys, in this case Inconel 718. Both tools are made of cemented carbide grades with binder content in the range of 3 to 10 wt%. However, Tool A has a submicron grade, indicating that its grain size is below 1 μm, while Tool B has an ultrafine grade, with a grain size larger than 1 μm. Despite these differences, both tools exhibit exceptionally high wear resistance and reliability against breakage, making them suitable samples for comparison in the investigation. According to the general parameter to work with Inconel 718, the Vc established for this tools is about 20 m/min, using straight cutting oil to cool and lubricate the cutting area. Fig. 6 shows the approximate geometry of the tools and Table 1 details its characteristics.

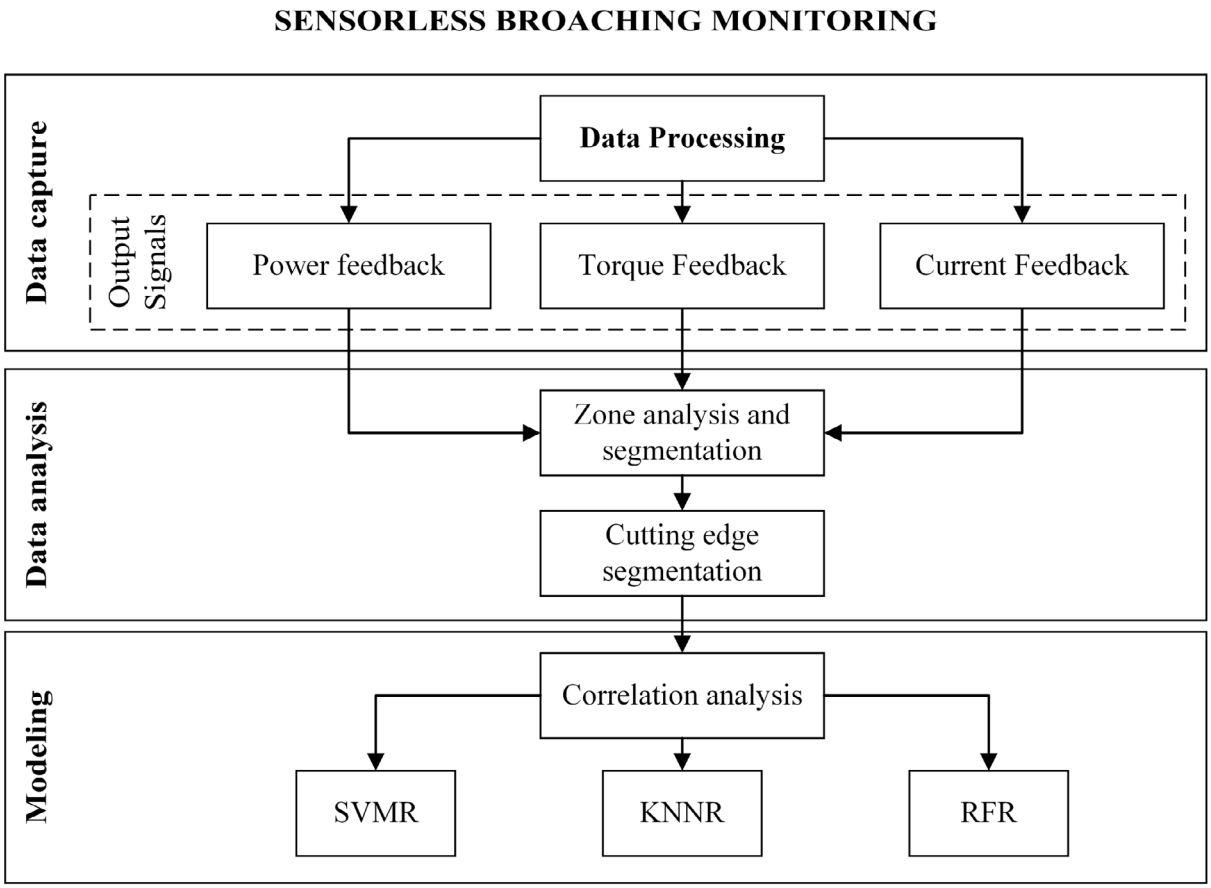

Fig. 7. Flowchart of the proposed method.

Table 1
Broaching tools general characteristic.

Tool	P (mm)	h (mm)	α (°)	γ (°)	L (mm)	H (mm)	R_1 (mm)	R_2 (mm)	R_β (μm)	Z (edges)
A	9–11	0.050–0.080	6–9	2–5	3–5	3–5	2–5	2–5	20–50	24
B	9–11	0.050–0.080	6–9	2–5	3–5	3–5	2–5	2–5	20–50	24

3. Method

This section explains the process of building a model based on the signals obtained in the trials and the tool flank wear that occurs during manufacturing. A schematic representation of the method is shown in Fig. 7.

The proposed method is divided into three sections: Data capture, Data analysis, and Modeling. The first step is to process the raw data from the datalogger to converted it into a more appropriate format for analysis, resulting in greater consistency and the correction of any discrepancies. This is followed by an examination of the signals to observe what information they provide about the broaching process and to decide which of them will be used for tool wear modeling.

Afterwards, the signals are then segmented into zones that reflect various aspects of the broaching process. A zone analysis is performed to understand the machine's behavior and obtain indicators that represent the process. Additionally, the dataset is divided to assess the influence of each cutting edge on the process, leading to the creation of a series of models that estimate the flank wear of each cutting edge of the broaching tool. Prior to modeling, a correlation analysis is conducted to confirm the relationship between the signals and the evolution of broaching tool wear. Once the correlation has been established, several predictive models are applied to detect broaching tool wear using only the machine data. Based on the size and characteristics of the dataset, the following regression algorithms are used from the Python scikit-learn package [33]:

- K-Nearest Neighbors Regressor (KNNR): Finds the K nearest neighbors of a given data point, computes the average of the target values of these neighbors, and uses this average as the prediction for the target value of the data point [33,34].

- Support Vector Machine Regressor (SVMR): Finds the best hyperplane: a plane that separates the input data into different regions in such a way that the mean squared error between the predicted values and the actual values is minimized [33,35].
- Random Forest Regressor (RFR): Builds multiple decision trees using randomly selected subsets of the data and features. Then, makes a prediction by averaging the predictions of individual trees [33,36].

The standardization and low variability among cutting tools allows us to model the evolution of the process using the large number of data collected during broaching. Therefore, the authors decided to use non-parametric algorithms. The authors used the slot number, power, current, and torque as input features for the predictor vector $\boldsymbol{x}$, and the tool wear as the output variable y.

The KNNR estimates the tool wear by averaging the outcome over the k nearest neighbors; to select the neighbors, the authors used the ℓ^1 distance function $\|\boldsymbol{x}_1 - \boldsymbol{x}_2\|_1 = \sum_i |x_{1,i} - x_{2,i}|$. If $\boldsymbol{x}$ is a new measure and $\{\boldsymbol{x}_j\}_{j=1,\dots,k}$ are the nearest neighbors of $\boldsymbol{x}$, then the estimated tool wear $\hat{y}$ is See [37, Sec. 2.3.2].

$$\hat{y}(\boldsymbol{x}) = \frac{1}{k}\sum_{j=1}^{k} y(\boldsymbol{x}_j).$$

The SVR is a regression method where the predictor space $\mathbb{R}^D$ is mapped to a high-dimensional space where the linear regression may better adjust the data. If the mapping is $\varphi : \mathbb{R}^D \to \mathbb{R}^M$, where M is larger than the number of data points, then the fitting function is

$$\hat{y}(\boldsymbol{x}) = \boldsymbol{\beta} \cdot \varphi(\boldsymbol{x}) + \beta_0.$$

Even though the new predictor space has larger dimension, computations are handle efficiently because the minimization problem only involves the kernel function $K(\boldsymbol{x}_1, \boldsymbol{x}_2) = \varphi(\boldsymbol{x}_1) \cdot \varphi(\boldsymbol{x}_2)$. The authors used the radial basis function kernel $K(\boldsymbol{x}_1, \boldsymbol{x}_2) = \exp(-\|\boldsymbol{x}_1 - \boldsymbol{x}_2\|^2/(2\sigma^2))$ and the ε-loss function with $\varepsilon = 0.1$, so there is no penalty for data within an ε distance from $\hat{y}$; see [37, Sec. 12.3.6]. The RFR grows B trees ($B = 36$ in our case) and average the value over them:

$$\hat{y}(\boldsymbol{x}) = \frac{1}{B}\sum_{b=1}^{B} T(\boldsymbol{x}; \theta_b),$$

where θ_b represents the process that generates the tree. Each tree is a piece-wise constant function, which is generated by randomly choosing a subset of variables, and cutting the space into halves several times until some stopping criterion is reached [37, Ch. 15].

4. Results and discussion

4.1. Data capture

As mentioned before, the signals of both servomotors are obtained through the CNC software as a series of CSV type files, each representing a broaching stroke. Several cleaning and homogenization procedures are performed on the broaching datasets, such as eliminating duplicate values, correcting residual values, and discarding empty strokes. Then, the true signal of the variables is obtained by summing the signals of both servomotors.

Once the data is processed, a variable analysis is performed to identify the most significant variables for estimating tool wear during the broaching process. Three variables are analyzed: power, current and torque feedback. These variables are the most significant to the broaching process out of all the datalogger variables, as they are the ones closest to the cutting force, which, as mentioned by Axinte and Gindy [3], is a signal sensitive to tool condition. These signals are plotted as a function of the Z position rather than time, since the position of the broach at Z is the same for all broaching strokes. This allows for a more accurate comparison of the signals and identification of the one that offers the best information about the process.

Fig. 8 shows these signals, indicating that the torque, power, and electrical current signals reach maximums of around 60 N m, 0.4 kW, and 15 A, respectively. This figure shows a random broaching stroke of the Tool A trial, which is representative of any of the broaching strokes for either tool. The torque variable has a higher frequency than the power and current variables, and consequently, the torque signal reflects more intricate details about the broaching process. The torque signal comprises approximately 4000 points per broaching stroke, while the power and electrical current signals contain around 800 points per broaching stroke. Therefore, the torque signal is the most suitable signal for additional analysis.

4.2. Data analysis

To explain the broaching process, a signal of a full broaching stroke, the same as Fig. 8, is shown in Fig. 9(a) where the torque signal is divided into six zones:

Zone 1: As the workpiece begins to lift, an acceleration is required to initiate the broaching stroke, resulting in a torque peak of approximately 50 Nm.

Zone 2: As the workpiece moves up the column at a consistent pace, the torque remains constant at 30 Nm.

Zone 3: Broaching starts,so the torque peaks to 60 Nm to sustain the Vc.

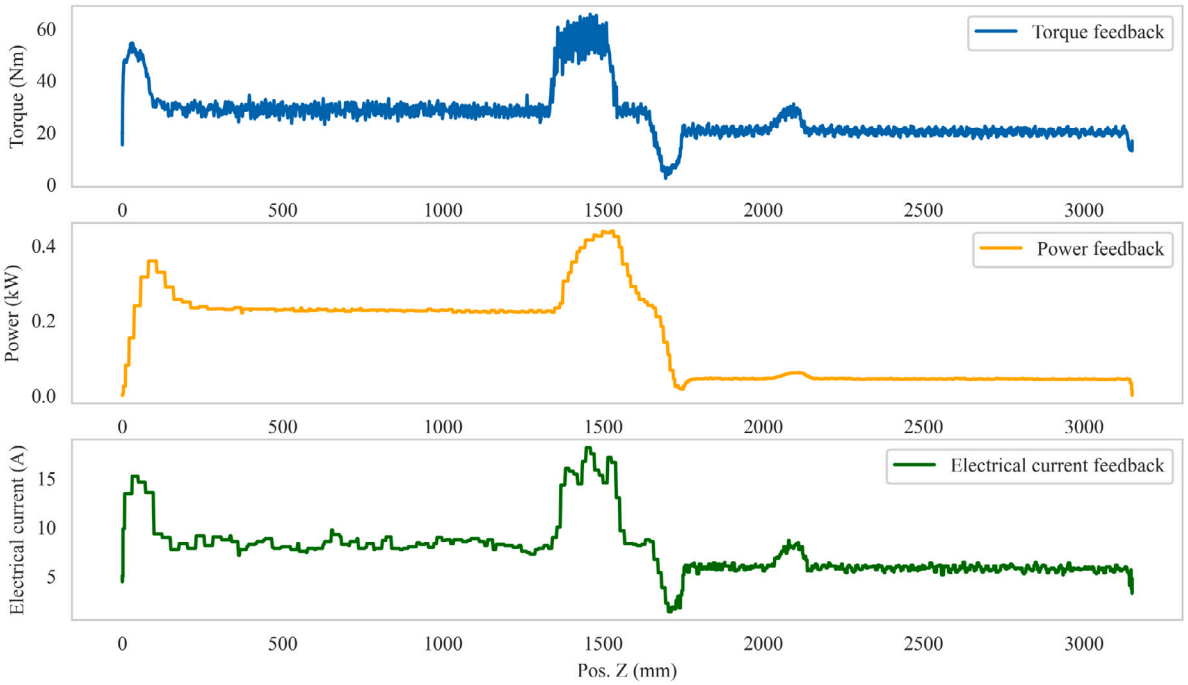

Fig. 8. Torque, power and current feedback in a broaching stroke.

Zone 4: As shown in Fig. 1, another broaching tool, named cleaner in the Figure, is found on the column after the main broaching tool to widen the existing slot. This broaching is done at a lower Vc, so in order to slow down, the torque done by the servo-motors sinks.

Zone 5: Once the new Vc is achieved, the torque peaks again when the widening tool enters the workpiece.

Zone 6: The torque remains constant at 20 Nm until the end of the stroke.

Furthermore, when enlarging the graph in the main broaching area (Zone 3) Fig. 9(b), a series of equidistant peaks appear in the image, following the tool's shape. These peaks are the points at which the workpiece contacts the cutting edges of the broaching tool, allowing one to see the effect of each cutting edge on the broaching process. It is notable that Zone 3 has a growing, a stable and an ending phase. Due to this, the broaching zone is divided into three zones, which are displayed in Fig. 9(b).

Start zone: The broaching starts and the cutting edges contact the workpiece, so the torque increases gradually from approximately 30 Nm to 60 Nm as more cutting edges contact the disk.

Stable zone: Once the maximum number of cutting edges contact the workpiece, the torque becomes constant at 60 Nm as the number of cutting edges in contact remains stable.

End zone: The torque decreases to 30 Nm as the cutting edges exit the workpiece until the broaching stops.

Finally, Fig. 9(c) shows the torque in the Stable zone, ranging from approximately 50 to 65 Nm. The actual signal is compared with the estimated theoretical function of the cutting force during the broaching process. This shows that the torque signal has a sufficient sample rate to observe the impact of the contact of each cutting edge, which is crucial for further analysis.

After segmenting the dataset into the three defined zones, the next step is to analyze the evolution of the average torque in Zone 3 as shown in Fig. 10. This figure displays the evolution in the Tool A trial. It shows that there is no visible trend in the torque evolution of Zone 3. Therefore, Zone 2 is analyzed to see the evolution of the torque in the moments where no broaching is occurring. This evolution is shown in Fig. 10.

The non-constant evolution of the torque in Zone 2 indicates that the first graph in Fig. 10 does not represent the true torque evolution caused solely by the broaching process, but rather a combination of the torque induced by the machine error in torque measurements and the torque from the broaching process. Therefore, this error is subtracted, and the result of the corrected torque evolution is the one shown in the third graph of Fig. 10. This correction is also carried out for the Tool B trial.

As a follow-up, Fig. 11 shows the subtraction to the torque evolution of the Start, Stable and End zones of both tools. The most relevant conclusion from this step is that, in the broaching process, as tool wear increases, there is an increase in torque in

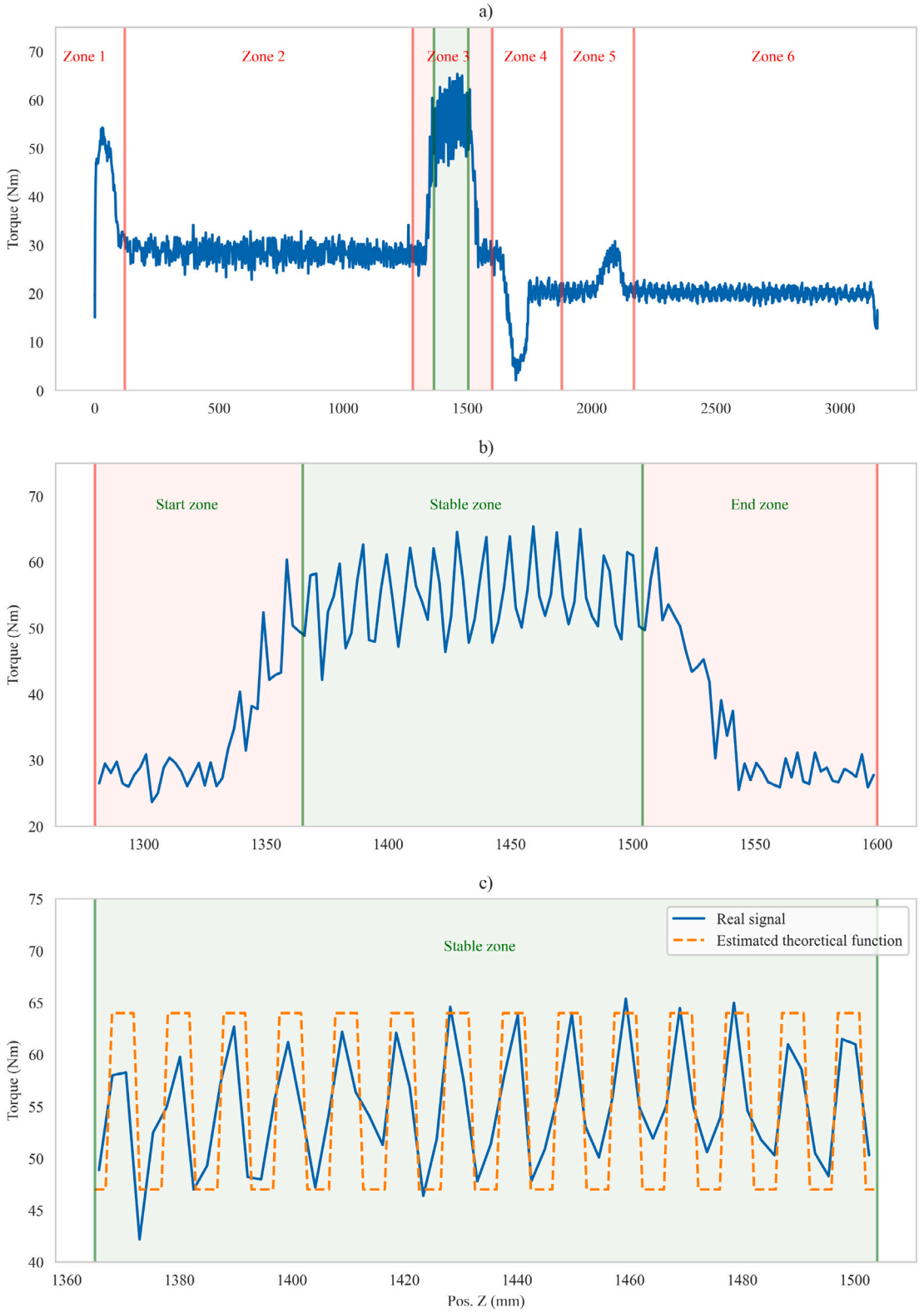

Fig. 9. (a) Zones of the torque signal of a full broaching stroke. (b) Zones of the torque signal in Zone 3. (c) Comparison between the actual torque signal and an estimated theoretical function of the cutting force.

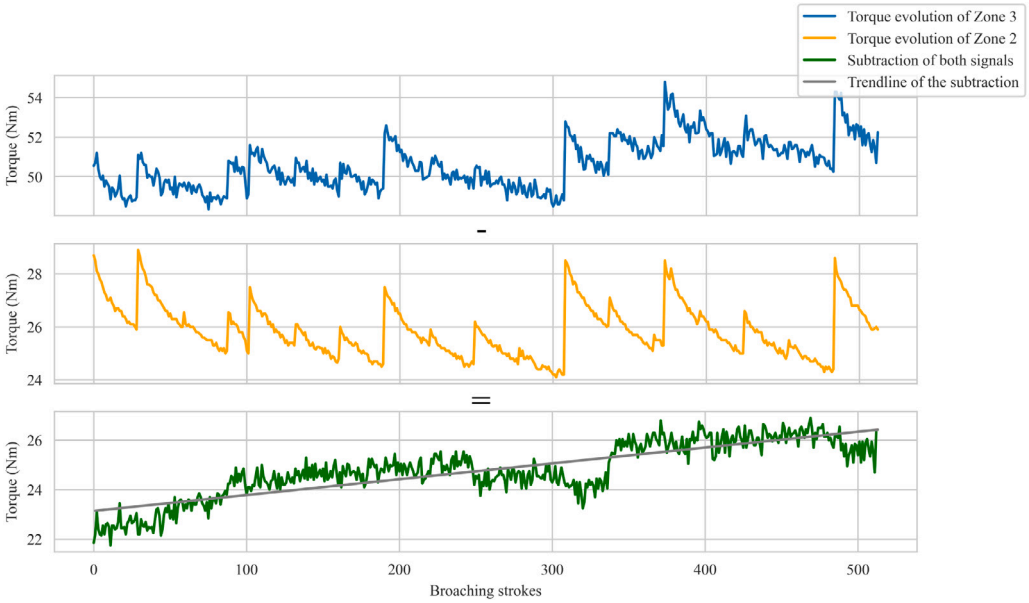

Fig. 10. Torque evolution of Zone 3 and Zone 2, and their subtraction with a trendline.

Fig. 11. Evolution of the torque in the start zone, stable zone and end zone for Tool A and Tool B.

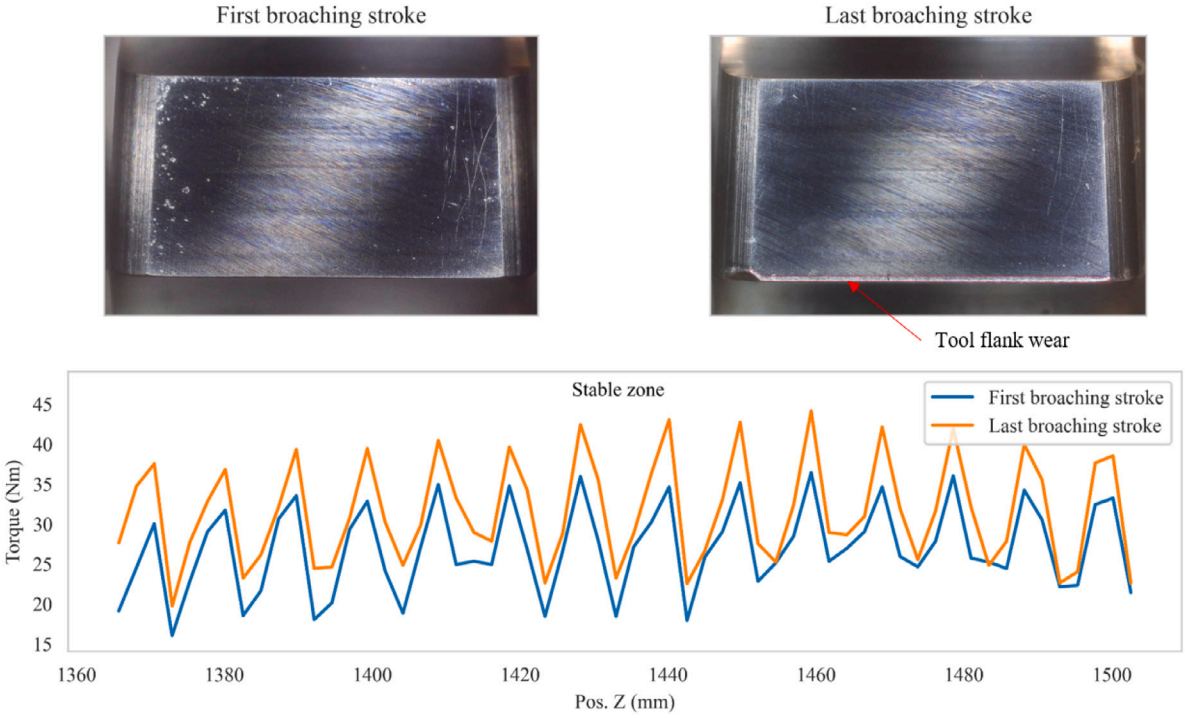

Fig. 12. Tool flank wear evolution and its effect on the torque signal.

the motors of approximately 4 Nm. Additionally, the torque evolution of the initial zone shows jumps resulting from the manual adjustment of the broaching stroke depth. This causes certain cutting edges to remain out of contact with the workpiece during some broaching strokes. The manual adjustment is carried out every complete turn of the disk, equating to every 89 passes, and it impacts the torque evolution of Zone 3. On the other hand, the torque evolution in the stable and end zone shows a noticeable trend of increasing with the number of broaching strokes.

4.3. Modeling

In addition to the machine data, broaching tool wear measurements were obtained using artificial vision techniques applied to the images of each cutting edge taken during the trials. Images were captured every 30 broaching strokes in both experiments, using a digital microscope camera. Various functions from the Python OpenCV library [38] were used to process the images, with the most relevant being the adaptive mean threshold, which emphasizes tool flank wear on the cutting edges. Using this approach, the tool flank wear area was calculated and then converted to the average tool flank wear.

The difference between a worn tool and a new one can be seen in Fig. 12, along with its effect on the torque signal. Using this tool wear data, the aim is to obtain a correlation between the evolution of the torque and the tool flank wear. To do this, the dataset is divided to obtain the evolution of the average torque in the impact zone of each tooth. To verify that a regressor model could yield favorable results, the Pearson correlation, a statistical measure that calculates the strength of the linear relationship between two continuous variables [39], was calculated between the torque evolution of each tooth and its tool wear. The results of the correlation are displayed in Fig. 13, and reveal a strong positive correlation, ranging from 0.4 to 0.8, between the evolution of torque in the servomotors and the flank wear in the tool. This correlation does not occur in the first cutting edges, because, as previously mentioned, the firsts cutting edges do not machine consistently or at all.

After obtaining the correlation and before applying these models, the datasets are divided into train data and test data, with a split of 80% train data and 20% test data. The data from both trials is merged so that the models have a larger dataset to train.

To select the model and tune its hyperparameters, the GridSearchCV function [33] is used to obtain the performance of a model for a grid of different hyperparameters. To compare the models, a metric must be chosen to evaluate them; the coefficient of determination, R^2 [40], is used. It should also be noted that this function cross-validates to obtain a more reliable model. The hyperparameter grid on which the models were evaluated is shown in Table 2.

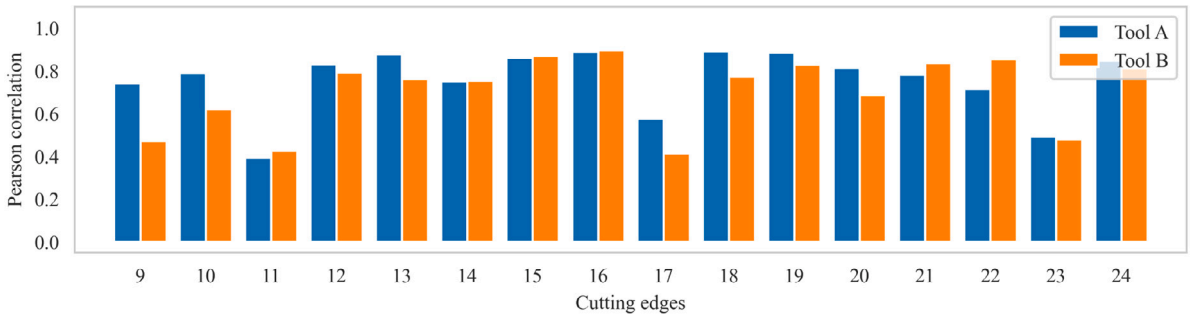

Fig. 13. Correlation between the evolution of the torque on each tooth and its tool flank wear in Tool A and Tool B.

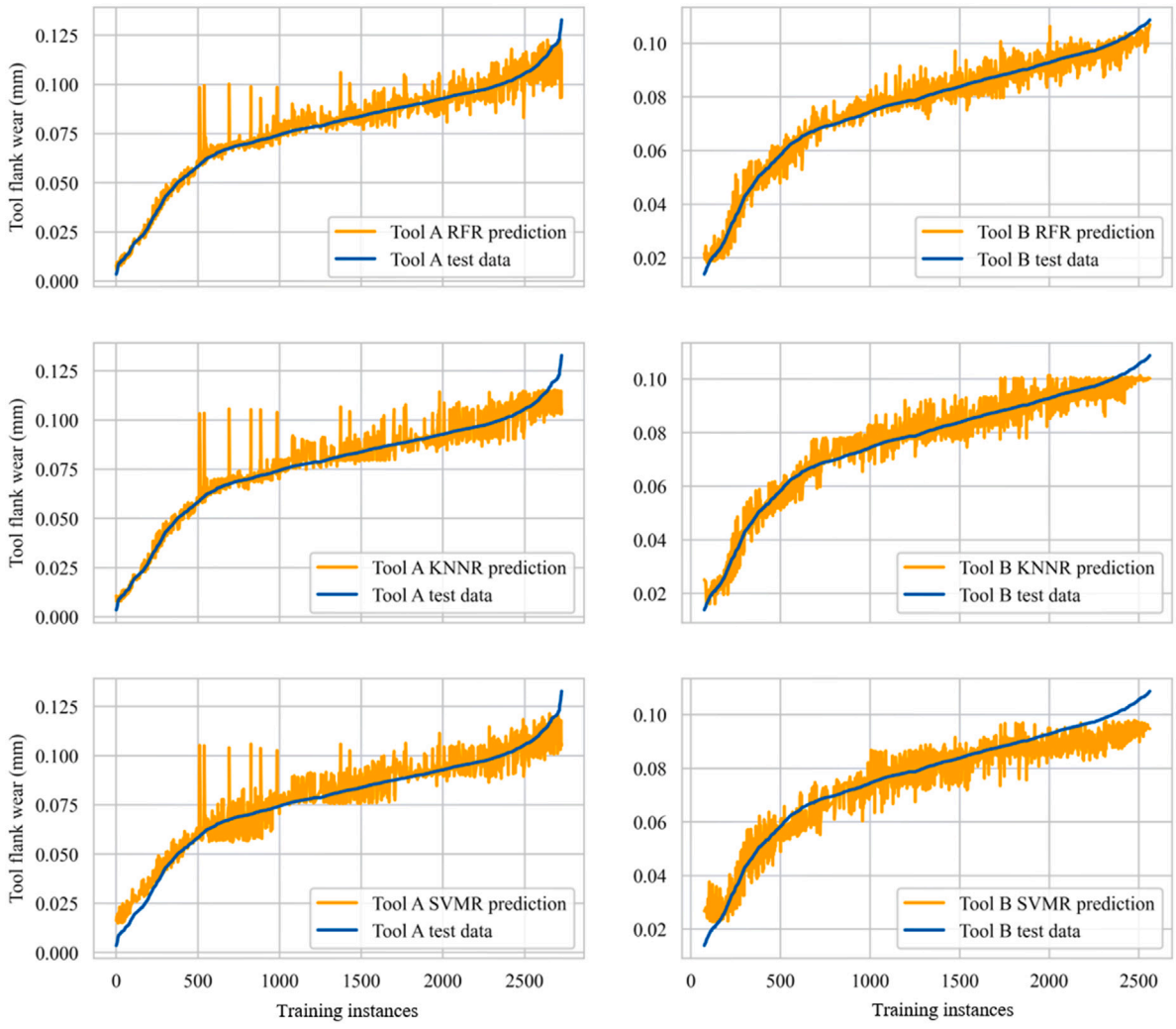

Fig. 14. Comparison between KNNR, RFR and SVMR prediction results on Tool A and Tool B, and actual tool wear data.

4.4. Results

Fig. 14 shows the results of the three models. These results have been obtained by fitting the test data on the pre-trained model with the optimal hyperparameters obtained with the GridSearchCV function. Regarding the visualization, the instances have been sorted from the lowest to the highest tool flank wear to obtain more precise graphs.

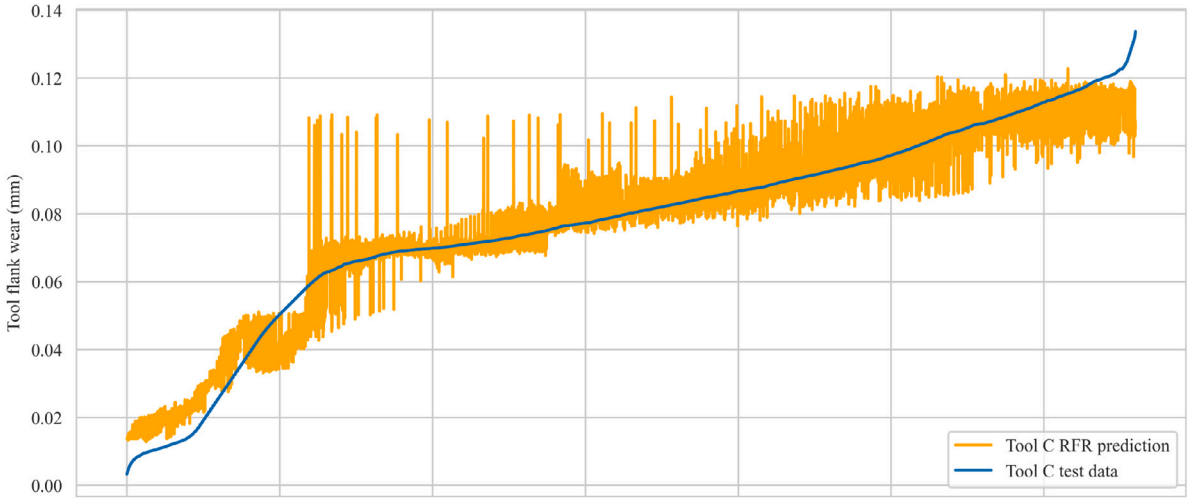

Fig. 15. Model validation — Tool C.

Table 2
Hyperparameters used in the models.

Model	1° Hyperparameter	2° Hyperparameter
RFR	N° of estimators: 36	Maximum depth: 13
KNNR	N° of neighbors : 46	Distance: Manhattan
SVMR	Kernel: RBF	–

Table 3
R^2, MAE, MSE and RMSE of the models.

Model	R^2	MAE	MSE	RMSE
RFR	0.966	0.00308	$2.14e^{-5}$	0.00463
KNNR	0.956	0.00369	$2.76e^{-5}$	0.00525
SVMR	0.925	0.00546	$4.68e^{-5}$	0.00684

All three models correctly match the predicted wear result to the measured wear. They all fit the initial and average wear values well, but the last instances with the highest wear are incorrectly predicted. This may be due to the lack of data for broaching strokes with high tool wear. The same pattern can be seen for each trial on the three models, which suggests that the prediction errors are related to the data from the trial. Of the three models, the RFR model is clearly the best fit along the entire curve for both trials. Additionally, several metrics are calculated for the different models, presented in Table 3.

According to the metrics, all models display highly accurate results, with a coefficient of determination greater than 0.9. However, as shown in Fig. 14, the RFR model has the highest accuracy, slightly surpassing the KNNR model. As expected, the SVMR model has the lowest accuracy among all the models, with a coefficient of determination of 0.925. Overall, the accuracy of the three models could be improved by increasing the computational power available to train the models, as shown in Wu et al. [41].

Based on the findings presented in this section, it can be affirmed that a reliable indirect monitoring of broaching tool wear has been achieved. This approach extends the research shown in Del Olmo et al. [25], and achieves comparable results to studies such as Shi et al. [16], which shows minimal error between the predicted values and the real values using a SVM-based model, and Wu et al. [41], which achieves a coefficient of determination of 0.99 using random forests with paralell computing, while using a sensorless approach.

4.5. Validation of the results

The RFR model achieved the the best results in the training phase, so it was used for the final validation of the model. In this last validation, data obtained using another tool (Tool C) with similar characteristics was used. The same procedure as in the two previous trials was followed to obtain this dataset.

After loading the new data into the pre-trained model and plotting the actual and predicted data together, the results are shown in Fig. 15 and Table 4. Analyzing the generated errors, it can see that the mean absolute error (MAE) is 0.0057 mm. This MAE corresponds to a 13% error in the predicted measurements. Fig. 16 shows the actual wear value overlaid with the predicted wear value and the difference between them, displayed on the secondary axis. As can be seen, the trend of the predicted wear closely resembles the trend of the actual wear. Overall, the error is acceptable, although it increases in some areas.

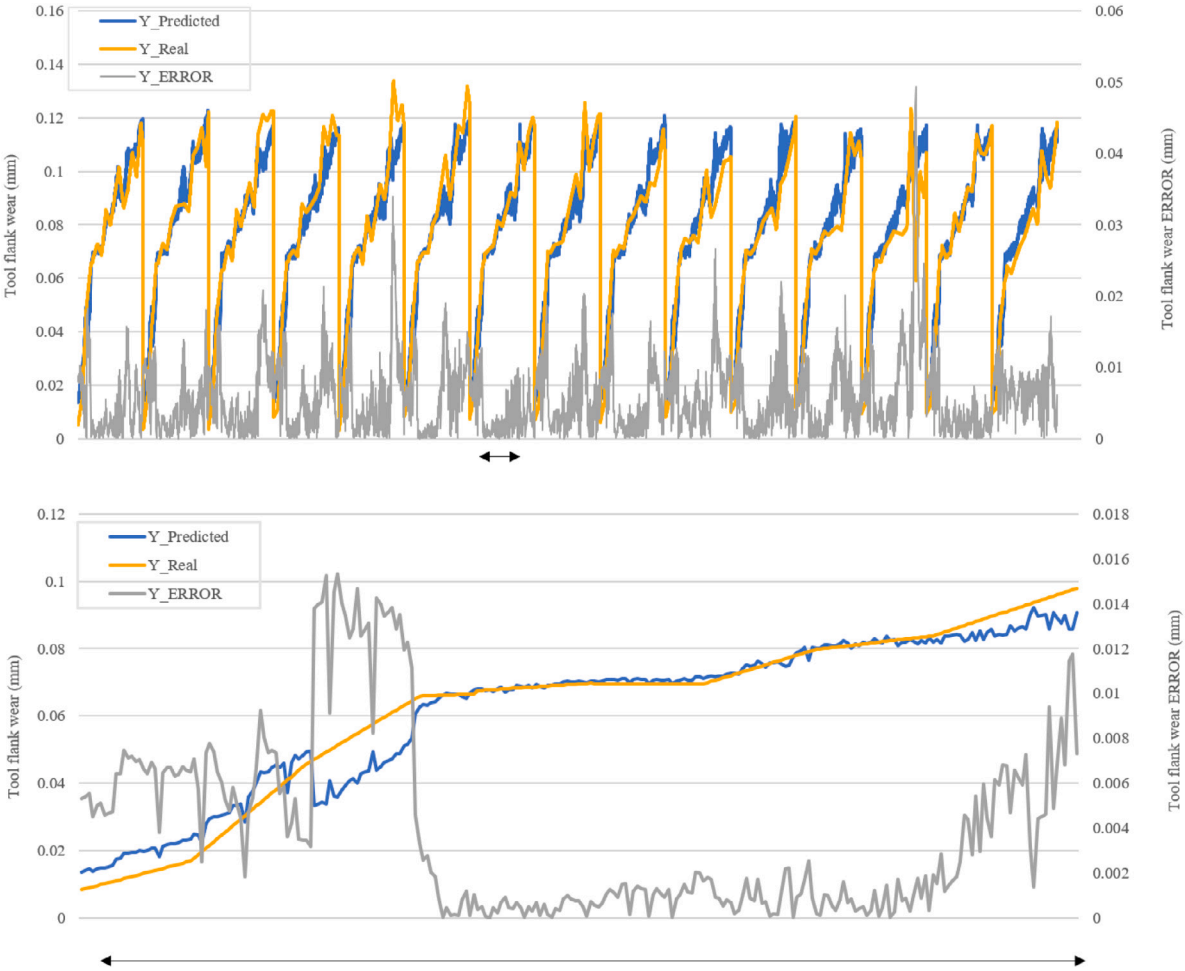

Fig. 16. Tool error — Tool C.

Table 4
R^2, MAE, MSE and RMSE of the models.

Tool	R^2	MAE	MSE	RMSE
Tool C	0.929	0.00568	$5.80e^{-5}$	0.00761

4.6. Discussion

This research introduces a novel, cost-effective and easier to implement method to model and predict tool wear in broaching tools. The method involves monitoring the broaching process by measuring the torque consumption of the servomotors in an electromechanical broaching machine.

The primary data collection method during the broaching process typically involves external devices, such as load cells, accelerometers, or AE sensors [3,13]. However, Bediaga et al. [42] have emphasized several challenges associated with these devices, including the need for calibration and maintenance to ensure accurate functionality, as well as difficulties in integrating them into the machine while maintaining process rigidity. Consequently, these factors limit their practicality for manufacturing industries aiming to control the production line, despite their high acquisition frequency and sensitivity compared to alternative monitoring methods such as power consumption.

As noted by Axinte & Gindy [3], the measurement of pressure signals was not considered for hydraulic power broaching machines due to the limitations of the hydraulic circuit design. However, they suggested that power consumption monitoring could be a viable option for mechanically powered broaching machines. This paper aligns with that line of research. Instead of using consumed power, it focuses on the torque consumed by the servomotors. This approach is chosen because other machine signals extracted by the CNC control are filtered, distorting the received signal and failing to reflect the true reality of the process. The main drawback is the

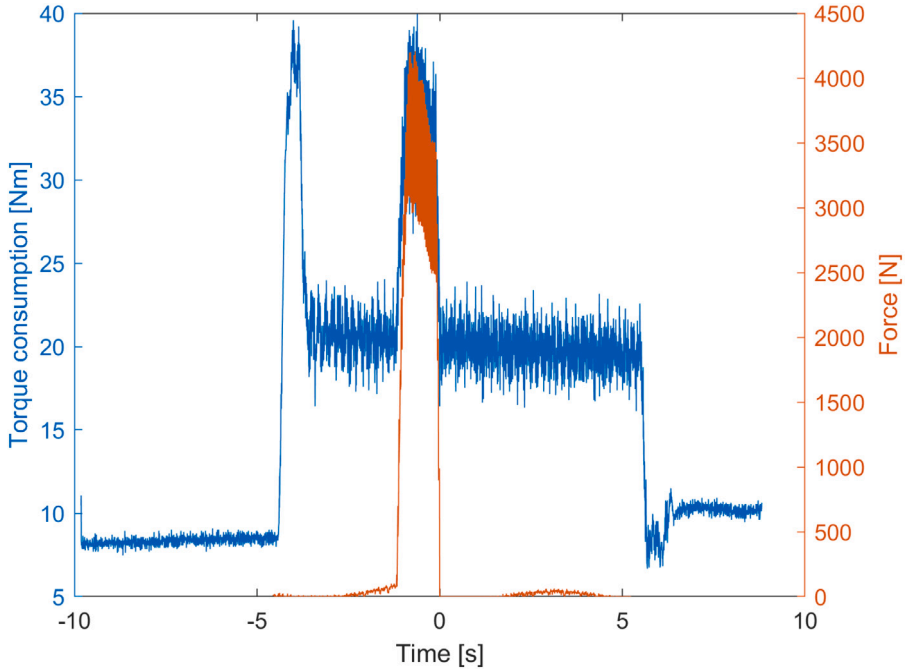

Fig. 17. Comparison between torque consumption (datalogger) and force signal (load cell sensor) — Broaching cycle.

lower acquisition frequency compared to more advanced devices. Nonetheless, a frequency of 250 Hz has been determined to be sufficient for the broaching process.

When selecting algorithms for generating a wear prediction model based on machine consumption signals, it is vital to identify promising candidates in this context. The achieved results align with those reported in the literature for other machining processes. Similar to Kilundu et al. [23], multiple algorithms were employed to determine the optimal choice, including RF, K-NN, and SVM. Among these, the RF algorithm displayed superior performance and yielded better results compared to the other two. On the other hand, the SVM algorithm encountered difficulties in adapting to the tool condition curve, particularly for initial values when the tool wear is low. This observation is consistent with findings from Benkedjouh et al. [22], who employed a data-driven model for milling operations using SVM algorithms.

For the research conducted by Del Olmo et al. [25], miniature integrated cell force sensors and piezoelectric triaxial accelerometers were installed in the electromechanical broaching machine. These sensors allowed for recording additional information about the broaching process at a significantly higher frequency than the machine's datalogger. This facilitated the discovery of more information for conducting various tooth-to-tooth process analyses and drawing conclusions, as described in the article. However, these sensors proved to be highly sensitive to the movement of the broaching plate, requiring extensive efforts in cleaning and pre-processing of the dataset. Moreover, calibration and installation of the sensors on the machine pose greater challenges due to the machine's configuration and the limited space between the cutting tool and the workpiece during broaching, which has been identified as a cause of tool breakages. Therefore, it is proposed to consider changing the sensor type in the future to mitigate these issues.

Regarding the relationship between motor torque signals and load cell measurements, as demonstrated in Fig. 17, analyzing the torque reading enables a comprehensive examination of the broaching cycle, encompassing the initial accelerations and the motor's efforts to maintain a constant cutting speed.

Additionally, Fig. 18 highlights that the magnitude recorded by the load cell sensor is lower than that captured by the machine's torque signal. This discrepancy could be attributed to challenges encountered while installing the sensor in proximity to the cutting point. Concerning the signal acquisition frequency of the sensors, despite exceeding the frequency at which the machine's control loop is monitored, the conducted research and obtained results consistently demonstrate that the measurement and prediction of tool wear can be reliably performed without requiring significantly higher sampling frequencies of the signals.

Regarding the variation of cutting parameters, broaching tools are designed to operate under predetermined parameters established by the manufacturer. Accordingly to Fabre et al. [6] increase in cutting speed affects the quality of the broached slot.

On the other hand, an increase in cutting speed would not allow for consistent and valuable data extraction with the sampling frequency available on the machine, necessitating the installation of additional sensors to capture the same information obtained through the machine's closed monitoring cycle.

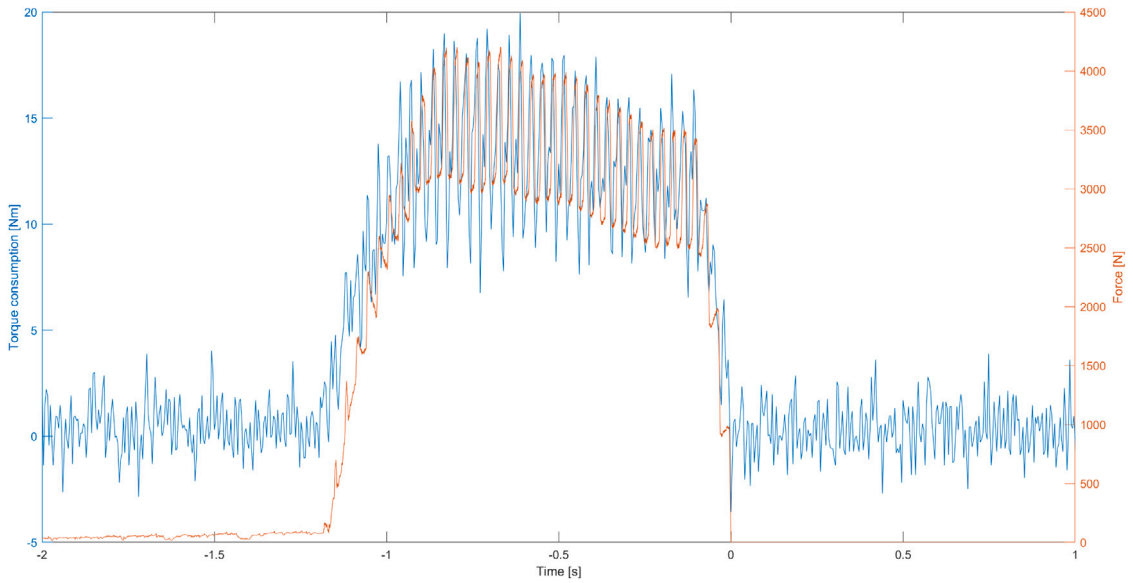

Fig. 18. Comparison between torque consumption (datalogger) and force signal (load cell sensor) — Cutting area.

5. Conclusions

The conclusions of this work are:

- The evolution of the torque signal extracted from the servomotors is closely related to the flank wear developed on the broaching tool during the machining process, even through the rack and pinion mechanism. Therefore, as the torque on the motors increases, the flank wear of the broach increases too.
- Regression machine learning algorithms can be effectively used for predicting tool wear, provided by machine data that has been properly preprocessed in order to avoid disturbances.
- The proposed method is sensorless, effective, inexpensive, and can be implemented directly in the CNC, as it is fed with information about the servomotor controller. However, it has some limitations, e.g., it does not capture all the information of the process, including vibrations or cutting forces during the broaching machine. Therefore, it is worthwhile to study ways to enhance monitoring through sensorization as a follow-up step.
- The method presented in this document can be expanded to include the characterization of various factors, such as different types of broaches, workpiece materials, and lubricants, among others.

CRediT authorship contribution statement

Iñigo Aldekoa: Conceptualization, Methodology, Investigation, Data analysis curation, Writing – original draft. **Ander del Olmo:** Conceptualization, Preliminary investigation, Writing – original draft. **Leonardo Sastoque-Pinilla:** Conceptualization, Methodology, Writing – review & editing. **Sara Sendino-Mouliet:** Investigation, Data analysis curation. **Unai Lopez-Novoa:** Conceptualization, Preliminary investigation, Supervision. **Luis Norberto López de Lacalle:** Conceptualization, Methodology, Supervision, Writing – review & editing.

Declaration of competing interest

The authors declare the following financial interests/personal relationships which may be considered as potential competing interests: Luis Norberto Lopez de Lacalle reports administrative support was provided by Artificial Intelligent Manufacturing for Sustainability Unit. Luis Norberto Lopez de Lacalle reports financial support was provided by Ministerio de Ciencia e Innovación de España. Unai Lopez-Novoa reports financial support was provided by Ministerio de Asuntos Económicos y Transformación Digital. Luis Norberto Lopez de Lacalle reports financial support was provided by Basque Government. Luis Norberto Lopez de Lacalle reports financial support was provided by Horizon Europe.

Data availability

The data that has been used is confidential.

Acknowledgments

The authors are grateful to PhD Jon Ander Ealo, PhD Felipe Ponce, Eng. Gonzalo Martínez de Pissón and PhD candidate Cristian Pérez-Salinas for providing valuable insight and support in this work. The authors want also to acknowledge the support received from the Artificial Intelligent Manufacturing for Sustainability Unit (AIMS) of the University of the Basque Country.

Thanks are addressed to MCIN/AEI/10.13039/501100011033/and European Union NextGenerationEU/ PRTR" - ≪Proyectos de Transición Ecológica y Transición Digital≫, *Quolink: A new way to assess quality in manufacturing processes by merging process data in high connected production systems in aeroturbines*, Ref TED2021-130044B-I00. Thanks are also addressed to Basque, Spain for the support of University research groups, grant IT1573-22. Thanks are also due to European commission by H2020 project n. 958357, and it is an initiative of the Factories-of-the-Future (FoF) Public Private Partnership, project *InterQ Interlinked Process, Product and Data Quality Framework for Zero-Defects Manufacturing*. Results were analyzed by models developed in Project KK-2022/0065 *Lanverso* and *Hatasu*.

This work was also partially supported by the Spanish *Ministerio de Asuntos Económicos y Transformación Digital* and the European Union *NextGenerationEU* through the project *LocoForge: Mimbres instantiation for railways and Industry 5.0 vertical sectors* (grant TSI-063000- 2021-47), funded by the Plan for Recovery, Transformation and Resilience.

References

[1] F. Klocke, P. Vogtel, S. Gierlings, D. Lung, D. Veselovac, Broaching of Inconel 718 with cemented carbide, Prod. Eng. 7 (6) (2013) 593–600, http://dx.doi.org/10.1007/s11740-013-0483-1.

[2] P.J. Arrazola, J. Rech, R. M'Saoubi, D. Axinte, Broaching: Cutting tools and machine tools for manufacturing high quality features in components, CIRP Ann. 69 (2) (2020) 554–577, http://dx.doi.org/10.1016/j.cirp.2020.05.010.

[3] D.A. Axinte, N. Gindy, Tool condition monitoring in broaching, Wear 254 (3) (2003) 370–382, http://dx.doi.org/10.1016/S0043-1648(03)00003-6, URL https://www.sciencedirect.com/science/article/pii/S0043164803000036.

[4] J. Loizou, W. Tian, J. Robertson, J. Camelio, Automated wear characterization for broaching tools based on machine vision systems, J. Manuf. Syst. 37 (2015) 558–563, http://dx.doi.org/10.1016/j.jmsy.2015.04.005.

[5] F. Boud, N.N.Z. Gindy, Application of multi-sensor signals for monitoring tool/workpiece condition in broaching, Int. J. Comput. Integr. Manuf. 21 (6) (2008) 715–729, http://dx.doi.org/10.1080/09511920701233357.

[6] D. Fabre, C. Bonnet, J. Rech, T. Mabrouki, Optimization of surface roughness in broaching, CIRP J. Manuf. Sci. Technol. 18 (2017) 115–127.

[7] M.J. Donachie, Titanium: A Technical Guide, ASM international, 2000.

[8] M. Kutz, Handbook of Materials Selection, John Wiley & Sons, 2002.

[9] M. Rahman, W. Seah, T. Teo, The machinability of inconel 718, J. Mater Process. Technol. 63 (1) (1997) 199–204, http://dx.doi.org/10.1016/S0924-0136(96)02624-6.

[10] D. Zhu, X. Zhang, H. Ding, Tool wear characteristics in machining of nickel-based superalloys, Int. J. Mach. Tools Manuf. 64 (2013) 60–77, http://dx.doi.org/10.1016/j.ijmachtools.2012.08.001.

[11] S. Mo, D. Axinte, T. Hyde, N. Gindy, An example of selection of the cutting conditions in broaching of heat-resistant alloys based on cutting forces, surface roughness and tool wear, J. Mater Process. Technol. 160 (3) (2005) 382–389, http://dx.doi.org/10.1016/j.jmatprotec.2004.06.026.

[12] D.A. Axinte, Approach into the use of probabilistic neural networks for automated classification of tool malfunctions in broaching, Int. J. Mach. Tools Manuf. 46 (12) (2006) 1445–1448, http://dx.doi.org/10.1016/j.ijmachtools.2005.09.017, URL https://www.sciencedirect.com/science/article/pii/S0890695505002701.

[13] E. Budak, Broaching process monitoring, in: Proceedings of Third International Conference on Metal Cutting and High Speed Machining, Metz-France, 2001, pp. 251–260.

[14] I. Bediaga, C. Ramirez, K. Huerta, C. Krella, J. Munoa, In-process tool wear monitoring in internal broaching, in: UMTIK 2016 - 17th International Conference on Machine Design and Production, Bursa, Turkey, 2016, URL https://hal.science/hal-01353881.

[15] X. Li, X. Liu, C. Yue, S.Y. Liang, L. Wang, Systematic review on tool breakage monitoring techniques in machining operations, Int. J. Mach. Tools Manuf. 176 (2022) 103882, http://dx.doi.org/10.1016/j.ijmachtools.2022.103882, URL https://www.sciencedirect.com/science/article/pii/S0890695522000335.

[16] D. Shi, D.A. Axinte, N.N. Gindy, Development of an online machining process monitoring system: a case study of the broaching process, Int. J. Adv. Manuf. Technol. 34 (1) (2007) 34–46, http://dx.doi.org/10.1007/s00170-006-0588-1.

[17] F. Aggogeri, N. Pellegrini, F.L. Tagliani, Recent advances on machine learning applications in machining processes, Appl. Sci. 11 (18) (2021) http://dx.doi.org/10.3390/app11188764, URL https://www.mdpi.com/2076-3417/11/18/8764.

[18] Y. Zhang, K. Zhu, X. Duan, S. Li, Tool wear estimation and life prognostics in milling: Model extension and generalization, Mech. Syst. Signal Process. 155 (2021) 107617, http://dx.doi.org/10.1016/j.ymssp.2021.107617, URL https://www.sciencedirect.com/science/article/pii/S0888327021000121.

[19] C.-H. Lee, J.-S. Jwo, H.-Y. Hsieh, C.-S. Lin, An intelligent system for grinding wheel condition monitoring based on machining sound and deep learning, IEEE Access 8 (2020) 58279–58289, http://dx.doi.org/10.1109/ACCESS.2020.2982800.

[20] D. Wu, C. Jennings, J. Terpenny, R.X. Gao, S. Kumara, A comparative study on machine learning algorithms for smart manufacturing: Tool wear prediction using random forests, J. Manuf. Sci. Eng. 139 (7) (2017) 071018, http://dx.doi.org/10.1115/1.4036350, arXiv:https://asmedigitalcollection.asme.org/manufacturingscience/article-pdf/139/7/071018/6405639/manu_139_07_071018.pdf.

[21] S. Cho, S. Asfour, A. Onar, N. Kaundinya, Tool breakage detection using support vector machine learning in a milling process, Int. J. Mach. Tools Manuf. 45 (3) (2005) 241–249, http://dx.doi.org/10.1016/j.ijmachtools.2004.08.016, URL https://www.sciencedirect.com/science/article/pii/S0890695504001993.

[22] T. Benkedjouh, K. Medjaher, N. Zerhouni, S. Rechak, Health assessment and life prediction of cutting tools based on support vector regression, J. Intell. Manuf. 26 (2015) 213–223.

[23] B. Kilundu, P. Dehombreux, X. Chiementin, Tool wear monitoring by machine learning techniques and singular spectrum analysis, Mech. Syst. Signal Process. 25 (1) (2011) 400–415, http://dx.doi.org/10.1016/j.ymssp.2010.07.014, URL https://www.sciencedirect.com/science/article/pii/S0888327010002505.
[24] M.E. Korkmaz, M.K. Gupta, Z. Li, G.M. Krolczyk, M. Kuntoğlu, R. Binali, N. Yaşar, D.Y. Pimenov, Indirect monitoring of machining characteristics via advanced sensor systems: a critical review, Int. J. Adv. Manuf. Technol. 120 (11) (2022) 7043–7078, http://dx.doi.org/10.1007/s00170-022-09286-x.
[25] A. del Olmo, L. López de Lacalle, G. Martínez de Pissón, C. Pérez-Salinas, J. Ealo, L. Sastoque, M. Fernandes, Tool wear monitoring of high-speed broaching process with carbide tools to reduce production errors, Mech. Syst. Signal Process. 172 (2022) 109003, http://dx.doi.org/10.1016/j.ymssp.2022.109003.
[26] C.F. Pérez-Salinas, A. del Olmo, L.N. López de Lacalle, Estimation of drag finishing abrasive effect for cutting edge preparation in broaching tool, Materials 15 (15) (2022).
[27] T. Bergs, G. Smeets, M. Seimann, B. Doebbeler, A. Klink, F. Klocke, Surface integrity and economical assessment of alternative manufactured profiled grooves in a nickel-based alloy, Procedia Manuf. 18 (2018) 112–119, http://dx.doi.org/10.1016/j.promfg.2018.11.015, 18th Machining Innovations Conference for Aerospace Industry, MIC 2018, 28-29 December 2018, Garbsen Germany.
[28] N. Miloslavskaya, A. Tolstoy, Big data, fast data and data lake concepts, Procedia Comput. Sci. 88 (2016) 300–305, http://dx.doi.org/10.1016/j.procs.2016.07.439, 7th Annual International Conference on Biologically Inspired Cognitive Architectures, BICA 2016, held July 16 to July 19, 2016 in New York City, NY, USA.
[29] J.P. Usuga Cadavid, S. Lamouri, B. Grabot, R. Pellerin, A. Fortin, Machine learning applied in production planning and control: a state-of-the-art in the era of industry 4.0, J. Intell. Manuf. 31 (6) (2020) 1531–1558, http://dx.doi.org/10.1007/s10845-019-01531-7.
[30] Savvy data systems, 2023, https://www.savvydatasystems.com/es/inicio, Accessed: 2023-03-06.
[31] A. Chamanfar, L. Sarrat, M. Jahazi, M. Asadi, A. Weck, A. Koul, Microstructural characteristics of forged and heat treated Inconel-718 disks, Mater. Des. (1980-2015) 52 (2013) 791–800, http://dx.doi.org/10.1016/j.matdes.2013.06.004.
[32] D. Thakur, B. Ramamoorthy, L. Vijayaraghavan, Study on the machinability characteristics of superalloy Inconel 718 during high speed turning, Mater. Des. 30 (5) (2009) 1718–1725, http://dx.doi.org/10.1016/j.matdes.2008.07.011.
[33] F. Pedregosa, G. Varoquaux, A. Gramfort, V. Michel, B. Thirion, O. Grisel, M. Blondel, P. Prettenhofer, R. Weiss, V. Dubourg, et al., Scikit-learn: Machine learning in Python, J. Mach. Learn. Res. 12 (2011) 2825–2830.
[34] L. Devroye, L. Gyorfi, A. Krzyzak, G. Lugosi, On the strong universal consistency of nearest neighbor regression function estimates, Ann. Statist. 22 (3) (1994) 1371–1385, http://dx.doi.org/10.1214/aos/1176325633.
[35] S.R. Gunn, et al., Support Vector Machines for Classification and Regression, ISIS Technical Report, 14 (1), 1998, pp. 5–16.
[36] U. Grömping, Variable importance assessment in regression: Linear regression versus random forest, Amer. Statist. 63 (4) (2009) 308–319, http://dx.doi.org/10.1198/tast.2009.08199.
[37] T. Hastie, R. Tibshirani, J. Friedman, The Elements of Statistical Learning, second ed., in: Springer Series in Statistics, Springer, New York, 2009, p. xxii+745, http://dx.doi.org/10.1007/978-0-387-84858-7, Data mining, inference, and prediction.
[38] G. Bradski, The opencv library, Dr. Dobb's J. Softw. Tools (2000).
[39] I. Cohen, Y. Huang, J. Chen, J. Benesty, J. Benesty, J. Chen, Y. Huang, I. Cohen, Pearson correlation coefficient, Noise Reduct. Speech Process. (2009) 1–4.
[40] N.J. Nagelkerke, et al., A note on a general definition of the coefficient of determination, Biometrika 78 (3) (1991) 691–692.
[41] D. Wu, C. Jennings, J. Terpenny, S. Kumara, R.X. Gao, Cloud-based parallel machine learning for tool wear prediction, J. Manuf. Sci. Eng. 140 (4) (2018) http://dx.doi.org/10.1115/1.4038002.
[42] I. Bediaga, C. Ramirez, K. Huerta, C. Krella, J. Munoa, In-process tool wear monitoring in internal broaching, in: UMTIK 2016-17th International Conference on Machine Design and Production, 2016.